# ESO Phase 3 Data Release Description

| | |
|---|---|
| **Data Collection** | ATLASGAL |
| **Release Number** | 1 |
| **Data Provider** | Frederic Schuller, K. Immer, Y. Contreras, T. Csengeri, J. S. Urquhart |
| **Date** | 19.01.2016 |


## Abstract

The APEX Telescope Large Area Survey of the Galaxy (ATLASGAL) is an imaging survey covering 420 sq. deg. of the inner Galactic plane at a wavelength of 870 μm. The observations were carried out between 2007 and 2010, using the LABOCA bolometer array at the APEX telescope, located at 5100m in Llano de Chajnantor, in the Atacama desert. The noise level reached is typically 60 mJy/beam, with an angular resolution of 19''. In total, this survey required more than 400 hours of telescope time, which was shared between the Max-Planck-Institut, ESO, and Chile.

The continuum emission detected at this wavelength mostly originates from cold interstellar dust. These data reveal thousands of compact, dusty clumps, as well as the large-scale structure of the interstellar medium. The current release consists of emission maps covering the full area surveyed, split in 3x3 sq. deg. tiles. A second set of images, where the LABOCA data have been combined with the results of the Planck satellite, is also available. In addition, two compact source catalogs, extracted with two different methods, are provided. These data are also available, with complementary information, from the ATLASGAL web page at the Max-Planck-Institut für Radioastronomie: http://atlasgal.mpifr-bonn.mpg.de


## Overview of Observations

The data taken as part of the ATLASGAL survey were observed in a total of 732 on-the-fly maps. These data have been reduced, calibrated, and combined in order to produce 3x3 sq. deg. tiles covering the range from -80º to +60º in Galactic longitude. The distribution of the 47 resulting tiles is shown in Fig. 1.

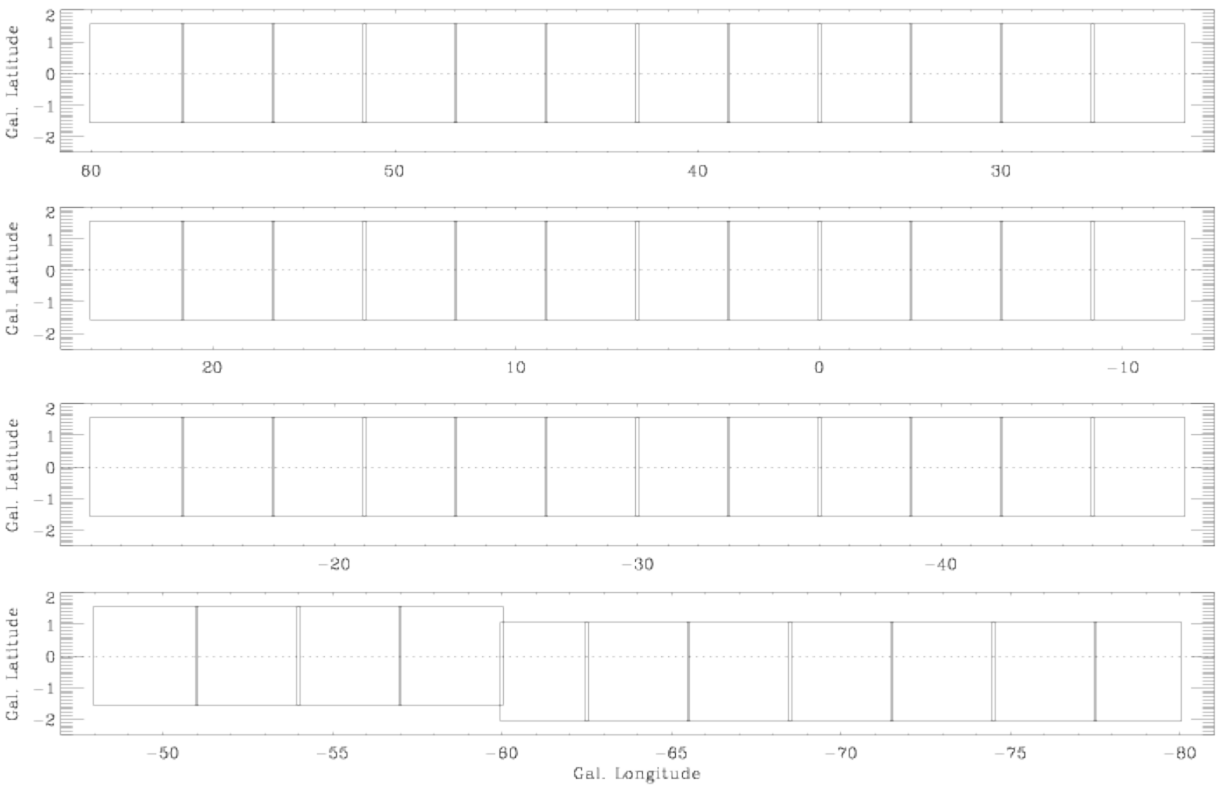


*Fig. 1: The distribution of all 3x3 sq. deg. tiles composing the ATLASGAL data release is shown in Galactic coordinates.*

## Release Content

The full survey coverage has been split into 47 3x3 sq. deg. tiles, as shown in Fig. 1. The table below lists the central position (in Galactic longitude and in Equatorial coordinates) and the extent (in Galactic coordinates) of each tile.

| $l_0$ | R.A. [J2000] | Dec [J2000] | $l_{min}$ | $l_{max}$ | $b_{min}$ | $b_{max}$ |
|---|---|---|---|---|---|---|
| -79.0 | 10:05:39.4 | -55:38:50 | -80.54 | -77.46 | -2.10 | +1.10 |
| -76.0 | 10:23:38.0 | -57:20:07 | -77.54 | -74.46 | -2.10 | +1.10 |
| -73.0 | 10:43:14.8 | -58:50:55 | -74.54 | -71.46 | -2.10 | +1.10 |
| -70.0 | 11:04:31.5 | -60:09:35 | -71.54 | -68.46 | -2.10 | +1.10 |
| -67.0 | 11:27:24.5 | -61:14:27 | -68.54 | -65.46 | -2.10 | +1.10 |
| -64.0 | 11:51:43.2 | -62:03:56 | -65.54 | -62.46 | -2.10 | +1.10 |
| -61.0 | 12:17:09.0 | -62:36:35 | -62.54 | -59.46 | -2.10 | +1.10 |
| -58.5 | 12:38:53.2 | -62:50:13 | -60.04 | -56.96 | -1.60 | +1.60 |
| -55.5 | 13:05:10.8 | -62:49:48 | -57.04 | -53.96 | -1.60 | +1.60 |
| -52.5 | 13:31:11.5 | -62:31:07 | -54.04 | -50.96 | -1.60 | +1.60 |
| -49.5 | 13:56:25.0 | -61:54:48 | -51.04 | -47.96 | -1.60 | +1.60 |
| -46.5 | 14:20:26.8 | -61:01:56 | -48.04 | -44.96 | -1.60 | +1.60 |
| -43.5 | 14:43:00.1 | -59:54:00 | -45.04 | -41.96 | -1.60 | +1.60 |
| -40.5 | 15:03:55.7 | -58:32:37 | -42.04 | -38.96 | -1.60 | +1.60 |
| -37.5 | 15:23:11.4 | -56:59:28 | -39.04 | -35.96 | -1.60 | +1.60 |
| -34.5 | 15:40:49.7 | -55:16:09 | -36.04 | -32.96 | -1.60 | +1.60 |
| -31.5 | 15:56:56.6 | -53:24:06 | -33.04 | -29.96 | -1.60 | +1.60 |
| -28.5 | 16:11:39.7 | -51:24:37 | -30.04 | -26.96 | -1.60 | +1.60 |
| -25.5 | 16:25:07.2 | -49:18:48 | -27.04 | -23.96 | -1.60 | +1.60 |
| -22.5 | 16:37:27.4 | -47:07:37 | -24.04 | -20.96 | -1.60 | +1.60 |
| -19.5 | 16:48:48.1 | -44:51:52 | -21.04 | -17.96 | -1.60 | +1.60 |
| -16.5 | 16:59:16.7 | -42:32:13 | -18.04 | -14.96 | -1.60 | +1.60 |
| -13.5 | 17:08:59.6 | -40:09:15 | -15.04 | -11.96 | -1.60 | +1.60 |
| -10.5 | 17:18:02.5 | -37:43:27 | -12.04 | -8.96 | -1.60 | +1.60 |
| -7.5 | 17:26:30.7 | -35:15:13 | -9.04 | -5.96 | -1.60 | +1.60 |
| -4.5 | 17:34:28.6 | -32:44:54 | -6.04 | -2.96 | -1.60 | +1.60 |
| -1.5 | 17:42:00.2 | -30:12:48 | -3.04 | +0.04 | -1.60 | +1.60 |
| +1.5 | 17:49:09.0 | -27:39:11 | -0.04 | +3.04 | -1.60 | +1.60 |
| +4.5 | 17:55:58.0 | -25:04:14 | +2.96 | +6.04 | -1.60 | +1.60 |
| +7.5 | 18:02:30.1 | -22:28:11 | +5.96 | +9.04 | -1.60 | +1.60 |
| +10.5 | 18:08:47.8 | -19:51:10 | +8.96 | +12.04 | -1.60 | +1.60 |
| +13.5 | 18:14:53.1 | -17:13:22 | +11.96 | +15.04 | -1.60 | +1.60 |
| +16.5 | 18:20:48.1 | -14:34:53 | +14.96 | +18.04 | -1.60 | +1.60 |
| +19.5 | 18:26:34.7 | -11:55:52 | +17.96 | +21.04 | -1.60 | +1.60 |
| +22.5 | 18:32:14.6 | -09:16:25 | +20.96 | +24.04 | -1.60 | +1.60 |
| +25.5 | 18:37:49.3 | -06:36:38 | +23.96 | +27.04 | -1.60 | +1.60 |
| +28.5 | 18:43:20.5 | -03:56:37 | +26.96 | +30.04 | -1.60 | +1.60 |
| +31.5 | 18:48:49.6 | -01:16:28 | +29.96 | +33.04 | -1.60 | +1.60 |
| +34.5 | 18:54:17.9 | +01:23:44 | +32.96 | +36.04 | -1.60 | +1.60 |
| +37.5 | 18:59:47.1 | +04:03:53 | +35.96 | +39.04 | -1.60 | +1.60 |
| +40.5 | 19:05:18.4 | +06:43:53 | +38.96 | +42.04 | -1.60 | +1.60 |
| +43.5 | 19:10:53.3 | +09:23:39 | +41.96 | +45.04 | -1.60 | +1.60 |
| +46.5 | 19:16:33.5 | +12:03:06 | +44.96 | +48.04 | -1.60 | +1.60 |
| +49.5 | 19:22:20.4 | +14:42:06 | +47.96 | +51.04 | -1.60 | +1.60 |
| +52.5 | 19:28:15.9 | +17:20:33 | +50.96 | +54.04 | -1.60 | +1.60 |
| +55.5 | 19:34:21.7 | +19:58:19 | +53.96 | +57.04 | -1.60 | +1.60 |
| +58.5 | 19:40:39.9 | +22:35:17 | +56.96 | +60.04 | -1.60 | +1.60 |

## Release Notes

A complete description of the ATLASGAL data reduction and calibration is given in Schuller et al. (2009). The method used to combine the Planck and ATLASGAL data together is described in Csengeri et al. (2016).

Two compact source catalogs have been extracted from the data: the Compact Source Catalogue (CSC), extracted with the SExtractor program (see Contreras et al. 2013 and Urquhart et al. 2014 for details); and the GaussClump Source Catalogue (GCSC, Csengeri et al. 2014), generated using the GaussClump program on maps where the extended emission component has been filtered out.

Both catalogues are included in this release. However, note that the GCSC is released as a single file, while the CSC consists of 47 files, i.e. one for each 3x3 sq. deg. tile of the survey (see details in section Data format below).

### Data Reduction and Calibration

The reduction of the LABOCA data has been done using the BoA software. The main steps in the data reduction include: flagging of bad or noisy bolometers; correlated sky-noise removal; de-spiking; baseline subtraction; and gridding of the data into a map. Finally, several on-the-fly maps overlapping on a given area are combined to produce the final maps.

The flux calibration has been done using two methods: the zenithal opacity at the wavelength of the observations is measured every 2-3 hours, using so-called "skydip" observations; this opacity is then used to scale the measured fluxes to their values "above" the atmosphere. In addition, primary calibrators (planets) as well as secondary calibrators (bright Galactic HII regions with known fluxes) are observed every 1-2 hours, between observations on the science targets, in order to correct for possible mis-calibration based on the sky opacity only. As a result, the uncertainty on the flux measurements is typically better than 15%.

The astrometry is also checked during the observations, by observing stars or quasars with well-known positions every 1-2 hours. As a result, the position uncertainty, as measured by the dispersion of the offsets measured on pointing sources, is generally below 4''.

### Data Quality

The rms noise level measured in the emission maps is in the range 50-80 mJy/beam in most parts of the survey. However, the noise varies from tile to tile due to several factors, including weather conditions and the number of times a given area was covered. The variation of the noise level with Galactic longitude is shown in Fig. 2. In particular, the innermost part of the Galactic plane ($|l| \leq 40^\circ$) benefitted from an extra coverage, resulting in a somewhat improved sensitivity. In addition, the noise level increases towards the lower and upper edge of the maps ($1^\circ \leq |b| \leq 1.5^\circ$), also as a result of the observing technique giving less integration there.

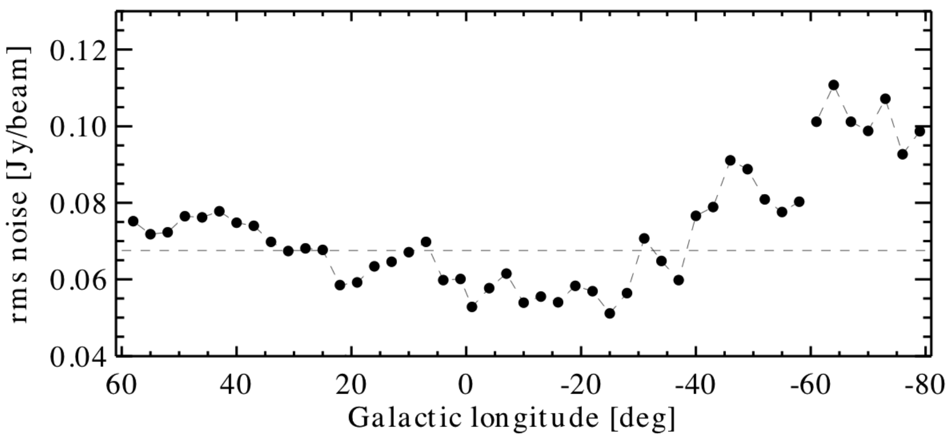


*Fig. 2: The rms noise level measured in each tile is plotted as a function of Galactic longitude. This rms has been determined by fitting a Gaussian to the distribution of the pixel values within $|b| \leq 1^\circ$. The horizontal dashed line indicates the average value (68 mJy/beam) for the main part of the survey ($|l| \leq 60^\circ$).*

### Known issues

Due to the removal of the emission coming from the sky, uniform emission at scales larger than ~2.5' is mostly filtered out in the ATLASGAL maps. The emission maps obtained by combining these data with the Planck data should recover the emission at all scales, from the LABOCA angular resolution (19'') upwards.

## Data Format

### Files Types

A total of six files are available for each position, as illustrated in the following example.

- ATLASGAL.49.5.fits : 2D map of the LABOCA emission
- ATLASGAL.49.5.weight.fits : associated weight map; this can be converted to an rms map using the equation: rms = 1/sqrt(weight)
- mr4_ATLASGAL.49.5.fits : map of the LABOCA emission where the emission on scales larger than 100'' has been filtered out (see Csengeri et al. 2014 for details)
- AG-Laboca-Planck.49.5.fits : map of the combined Planck + LABOCA data
- ATLASGAL_49_5_MASK_3.2sigma.fits : source maskresulting from the extraction with SExtractor
- ATLASGAL_49_5.ASC : catalogue file obtained from SExtractor

### Catalogue Columns

The catalogue files *.ASC, output from SExtractor, contain 23 columns, with the following definitions:

| Col. num. | Content | Description | Unit |
|---|---|---|---|
| 1 | NUMBER | Running object number | --- |
| 2 | X_WORLD | Barycenter position along world x axis | [deg] |
| 3 | Y_WORLD | Barycenter position along world y axis | [deg] |
| 4 | XPEAK_WORLD | World-x coordinate of the brightest pixel | [deg] |
| 5 | YPEAK_WORLD | World-y coordinate of the brightest pixel | [deg] |
| 6 | XPEAK_IMAGE | x-coordinate of the brightest pixel | [pixel] |
| 7 | YPEAK_IMAGE | y-coordinate of the brightest pixel | [pixel] |
| 8 | FLUX_AUTO | Flux within a Kron-like elliptical aperture | [count] |
| 9 | FLUXERR_AUTO | RMS error for AUTO flux | [count] |
| 10 | FLUX_RADIUS | Fraction-of-light radii | [pixel] |
| 11 | BACKGROUND | Background at centroid position | [count] |
| 12 | FLUX_MAX | Peak flux above background | [count] |
| 13 | ISOAREA_IMAGE | Isophotal area above Analysis threshold | [pixel^2] |
| 14 | THETA_IMAGE | Position angle (CCW/x) | [deg] |
| 15 | A_WORLD | Profile RMS along major axis (world units) | [deg] |
| 16 | B_WORLD | Profile RMS along minor axis (world units) | [deg] |
| 17 | THETA_WORLD | Position angle (CCW/world-x) | [deg] |
| 18 | ERRA_WORLD | World RMS position error along major axis | [pixel] |
| 19 | ERRB_WORLD | World RMS position error along minor axis | [pixel] |
| 20 | ERRTHETA_WORLD | Error ellipse pos. angle (CCW/world-x) | [deg] |
| 21 | FLAGS | Extraction flags | --- |
| 22 | ELONGATION | A_IMAGE/B_IMAGE | --- |
| 23 | ELLIPTICITY | 1 - B_IMAGE/A_IMAGE | --- |

In total, the SExtractor catalogues contain 10,163 compact sources, extracted from the whole 420 sq. deg. surveyed.

The GaussClump Source Catalog is provided as a single FITS file, named atlasgal_GCSC.fits. It contains 10,861 entries, with 10 columns, described in the table below.

| Col. num. | Content | Description | Unit |
|---|---|---|---|
| 1 | GC_ID | [1/10861] Sequential number of the source | --- |
| 2 | ATLAS_NAME | Name of the source (GLLL.llll+B.bbbb) | --- |
| 3 | RA | Right ascension (J2000) | deg |
| 4 | DE | Declination (J2000) | deg |
| 5 | MAJOR_FWHM | Beam convolved major axis of the fitted Gaussian | arcsec |
| 6 | MINOR_FWHM | Beam convolved minor axis of the fitted Gaussian | arcsec |
| 7 | PA | [-90/180] Position angle of the fitted Gaussian measured from north to east | deg |
| 8 | FLUX | Peak flux at 870 μm | Jy/beam |
| 9 | INT_FLUX | Integrated flux at 870 μm | Jy |
| 10 | SNR | Signal-to-noise ratio determined from the weight maps | --- |


## Acknowledgements

Please use the following statement in your articles when using these data:
Based on data products from observations made with the Atacama Pathfinder EXperiment (APEX), under ESO programme IDs 078.F-9040(A), 079.C-9501(A), 081.C-9501(A), 181.C-0885(A), 080.F-9701(A), 082.F-9701(A), 085.F-9505(A), and 085.F-9526(A). APEX is a collaboration between the Max-Planck-Institut für Radioastronomie, the European Southern Observatory, and the Onsala Space Observatory.


## References


Contreras, Y., Schuller, F., Urquhart, J. S., et al. 2013, A&A, 549, A45
Csengeri, T., Urquhart, J. S., Schuller, F., et al. 2014, A&A, 565, A75
Csengeri, T., Weiss, A., Wyrowski, F., et al. 2016, A&A, 585, A104
Schuller, F., Menten, K. M., Contreras, Y., et al. 2009, A&A, 504, 415
Urquhart, J. S., Csengeri, T., Wyrowski, F., et al. 2014, A&A, 568, A41